

A Practical Bandit Method with Advantages in Neural Network Tuning

Tianyu Wang^{*} Dawei Geng[†] Cynthia Rudin[‡]

Abstract

Stochastic bandit algorithms can be used for challenging non-convex optimization problems. Hyperparameter tuning of neural networks is particularly challenging, necessitating new approaches. To this end, we present a method that adaptively partitions the combined space of hyperparameters, context, and training resources (e.g., total number of training iterations). By adaptively partitioning the space, the algorithm is able to focus on the portions of the hyperparameter search space that are most relevant in a practical way. By including the resources in the combined space, the method tends to use fewer training resources overall. Our experiments show that this method can surpass state-of-the-art methods in tuning neural networks on benchmark datasets. In some cases, our implementations can achieve the same levels of accuracy on benchmark datasets as existing state-of-the-art approaches while saving over 50% of our computational resources (e.g. time, training iterations).

1 Introduction

The goal of many important real-world problems is to optimize an underlying function whose evaluation is expensive. Minimizing the number of times to query the underlying function is then desired. Problems of this kind include experimental design (Chaloner and Verdinelli, 1995; Srinivas et al., 2009; Martinez-Cantin, 2014), online recommendation (Ricci et al., 2015), data-efficient system control (Calandra et al., 2016; Lizotte et al., 2007; Mukadam et al., 2017), and tuning neural network hyperparameters (kernel size, pooling size, learning rate and its decay rate). Tuning hyperparameters of neural networks is not simply a gradient-free optimization problem, since some hyperparameter settings are significantly more expensive than others to be evaluated. When the user can control the computational resources dedicated to the tuning, algorithms within the stochastic bandit framework should be leveraging this control to obtain cost-effective performance, as is also suggested in the Bayesian Optimization setting (Kandasamy et al., 2017; Song et al., 2018).

A stochastic bandit problem assumes that payoffs are noisy and are drawn from a unchanging distribution. The study of stochastic bandit problems started with the discrete arm setting, where the agent is faced with a finite set of choices. Classic works on this problem date back to the Thompson Sampling problem (Thompson, 1933), Gittins index (Gittins, 1979), and some Upper Confidence Bound (UCB) methods (Lai and Robbins, 1985; Agrawal, 1995). Common solutions to this problem include the ϵ -greedy algorithms (Sutton and Barto, 1998), the UCB-based algorithms (Auer et al., 2002), and the Thompson Sampling algorithms (Agrawal and Goyal, 2012). These bandit strategies have led to powerful real-life applications. For example, Deep Q-Network (Mnih et al., 2015) uses ϵ -greedy for action exploration; and AlphaGO (Silver et al., 2016) uses UCT (Kocsis and Szepesvári, 2006), which is built on the UCB strategy, for action searching. One recent line of work on stochastic bandit problems considers the case where the arm space is infinite. In this setting, the arms are usually assumed to be in a subset of the Euclidean space (or a more general metric space), and the expected payoff function is assumed to be a function of the arms. Some works along this line model the expected payoff as a linear function of the arms (Auer, 2002; Dani et al., 2008; Li et al., 2010; Abbasi-Yadkori et al., 2011; Agrawal and Goyal, 2013; Abeille et al., 2017); some algorithms model the expected payoff as Gaussian processes over the arms (Srinivas et al., 2009; Contal et al., 2014; de Freitas et al., 2012; Vazquez and Bect, 2007); some algorithms assume that the expected payoff is a Lipschitz function of the arms (Slivkins, 2011; Kleinberg et al., 2008; Bubeck et al., 2011); and some assume locally Hölder payoffs on the real line (Auer et al., 2007). When the arms are continuous and equipped with a metric, and the expected payoff is Lipschitz continuous in the arm space, we

^{*}tianyu@cs.duke.edu, Department of Computer Science, Duke University

[†]dawei.geng@duke.edu, Department of Statistical Science, Duke University

[‡]cynthia@cs.duke.edu, Department of Computer Science and Department of Electrical and Computer Engineering, Duke University

refer to the problem as a stochastic Lipschitz bandit problem. In addition, when the agent’s decisions are made with the aid of contextual information, we refer to the problem as a contextual stochastic Lipschitz bandit problem. In this paper, we focus our study on the (contextual) stochastic Lipschitz bandit problems, and its application to neural network tuning. While our analysis focuses on the case of Lipschitz expected payoffs, our empirical results demonstrate that our methods can adapt to the landscape of the payoff and leverage properties other than Lipschitzness. This means our methods in practice have much better performance than analyses for Lipschitz bandit problems suggest. Few of the methods listed above consider computational resources as part of the algorithm, even though it is important for neural network tuning and other important problems.

Neural network tuning is challenging, and in recent years, the best performance has relied heavily on human tuning of the network’s hyperparameters. Given a training and validation set, the validation performance metric (e.g. validation accuracy) of the neural network can be viewed as a noisy function (payoff) of hyperparameters (arms), which include the architecture of the network, the learning rate, initialization, the number of training iterations, etc. This turns a neural network tuning problem into a stochastic bandit problem. The arms have different costs: if we train only for a small amount of iterations, we use less resources. Training for a small amount of iterations is often useful to judge initial conditions and architecture. Ideally, the method should be able to choose how long (how many iterations) to train in order to balance between exploration, exploitation, and cost of evaluation. As shown in Section 3, our methods balance between exploration, exploitation, and cost of evaluation for the problem of neural network tuning.

Our proposed algorithm, (Contextual) PartitionUCB, maintains a finite partition of the (context-)arm space and uses an Upper Confidence Bound strategy (Auer et al., 2002), as if the partition represents a finite set of (context-)arms. As we observe more data, the partition grows finer. To better deploy (Contextual) PartitionUCB to problems such as neural network tuning, we provide fast implementations using regression trees, since a regression tree corresponds to a partition. We show empirically that our proposed tuning methods outperform existing state-of-the-art on benchmark datasets. In summary, our contributions are twofold: **1)** we develop a novel stochastic Lipschitz bandit algorithm *PartitionUCB* and its contextual counterpart *Contextual PartitionUCB*. For compact domains in \mathbb{R}^d , both algorithms exhibit a $\tilde{O}(T^{\frac{d+1}{d+2}})$ regret bound with high probability; **2)** we develop *TreeUCB* (*TUCB*) and *Contextual TreeUCB* (*CTUCB*) as fast implementations of *PartitionUCB* and *Contextual PartitionUCB*. We apply TUCB and CTUCB to tuning neural networks. They can achieve a satisfactory level of accuracy as the average of existing state-of-the-art approaches while saving over 50% resource (e.g. time, total training iterations) on the MNIST dataset (LeCun, 1999), the SVHN dataset (Netzer et al., 2011) dataset and the CIFAR-10 dataset (Krizhevsky et al., 2012).

Related works: From a bandit perspective, the closest works are the Zooming bandit algorithm (and the contextual Zooming bandit algorithm) (Slivkins, 2011; Kleinberg et al., 2008) and the HOO algorithm (Bubeck et al., 2011), which inspired our work. Both the Zooming bandit algorithm and the HOO algorithm have excellent theoretical analyses, but suffer from practical inefficiency. The Zooming bandit algorithm (and the contextual Zooming bandit algorithm) keeps a cover of the arm space. As the Zooming bandit runs, some subsets in the cover shrink, resulting in some points of the arm space becoming uncovered. Once this happens, the algorithm needs to introduce new subsets of arms to maintain the cover. The operation of checking whether each arm is covered can be expensive and hard-to-implement in practice. The HOO algorithm does not require Zooming bandit’s covering oracle, but it is non-contextual. This makes it less general than the Contextual PartitionUCB algorithm. In addition, it requires a fine discretization of the arm space to start with. This initialization requirement makes HOO impractical, since problems like tuning neural networks can have arm spaces with millions of points in discrete spaces or infinite points in a parameter space. The practical efficiency of our method is partially a result of maintaining a careful partition of the space. This allows us to use a fast implementation of regression trees (Geurts et al., 2006).

Empirical results on tuning neural networks for the MNIST dataset (LeCun, 1999), the SVHN dataset (Netzer et al., 2011) dataset and the CIFAR-10 dataset (Krizhevsky et al., 2012), indicate that our methods tend to be more efficient and/or effective than 1) the state-of-the-art Bayesian optimization methods: the SPEARMINT package (Snoek et al., 2012) which integrates several Bayesian optimization methods (Swersky et al., 2013; Bergstra et al., 2011; Snoek et al., 2014; Snoek, 2013; Gelbart et al., 2014), the TPE algorithm (Bergstra et al., 2011) and the SMAC algorithm (Hutter et al., 2011); and 2) methods that focus explicitly on tuning neural networks: Hyperband algorithm (Li et al., 2016) (and SuccessiveHalving algorithm (Jamieson and Talwalkar, 2016)), the Harmonica algorithm (Hazan et al., 2017), and random search (Bergstra and Bengio, 2012). As suggested by the results in this paper, common bandit algorithms, such as UCB algorithms, can be competitive with the state-of-the-art methods for neural network tuning.

2 Algorithms

2.1 The PartitionUCB algorithm

Given a stochastic bandit problem, our goal is to locate the global maximum (minimum) of the payoff function via querying the payoff function at a sequence of points. The performance of the algorithm is typically measured by how quickly the algorithm is able to locate the maximum. In this paper, we focus our study on the following setting. A payoff function is defined over an arm space that is a compact subset $\mathcal{A} \subset \mathbb{R}^d$, and the payoff function of interest is $f : \mathcal{A} \rightarrow [0, 1]$ and the actual observations are given by $y(a) = f(a) + \epsilon$, where $\epsilon \sim \mathcal{N}(0, s^2)$.¹ For the theory, we assume that the payoff function f is Lipschitz in the sense that $\forall a, a' \in \mathcal{A}$, $|f(a) - f(a')| \leq c \|a - a'\|_\infty$ for some constant c . An agent is interacting with this environment in the following fashion. At each round t , based on past observations $(a_1, y(a_1), \dots, a_{t-1}, y(a_{t-1}))$, the agent makes a query at point a_t and observes the noisy payoff $y(a_t)$. The observation $y(a_t)$ is revealed only after the agent has made a decision a_t . The agent repeats this procedure with the goal of locating the maximum of f . To measure the performance of the agent's strategy, the concepts of regret and cumulative regret are defined. The regret at round t is defined to be

$$r_t = f(a^*) - f(a_t)$$

where a^* is the global maximizer of f ; and the cumulative regret up to time T is defined to be

$$R_T = \sum_{t=1}^T r_t.$$

The PartitionUCB algorithm runs by maintaining a sequence of adaptive finite partitions of the arm space. Intuitively, at each step t , PartitionUCB treats the problem as a finite-arm problem with respect to the partition bins at t . The partition bins become smaller and smaller as the algorithm runs. At each time t , we maintain partition $\mathcal{P}_t = \{P_t^{(1)}, \dots, P_t^{(k_t)}\}$ of the input space: for any t ,

$$\begin{cases} P_t^{(i)} \cap P_t^{(j)} = \phi, & \text{for } 1 \leq i < j \leq k_t \\ \bigcup_{j=1}^{k_t} P_t^{(j)} = \mathcal{A}. \end{cases} \quad (1)$$

Each bin in the partition is called a *region* and by convention $\mathcal{P}_0 = \mathcal{A}$.

Before formulating our strategy, we need to put forward several definitions. First of all, based on the partition \mathcal{P}_t at time t , we define an auxiliary function - the *Region Selection function*, in Definition 1 to aid our discussion.

Definition 1 (Region Selection function). *Given the partition \mathcal{P}_t , a function $p_t : \mathcal{A} \rightarrow \mathcal{P}_t$ is called a Region Selection function with respect to \mathcal{P}_t if for any $a \in \mathcal{A}$, $p_t(a)$ is the region in \mathcal{P}_t that contains a .*

For example, if the arm space $\mathcal{A} = [0, 2]$, and the partition $\mathcal{P}_t = \{[0, 1], [1, 2]\}$, then p_t is defined on $[0, 2]$ and

$$p_t(a) = \begin{cases} [0, 1], & \text{if } a \in [0, 1), \\ [1, 2], & \text{if } a \in [1, 2]. \end{cases}$$

As the name PartitionUCB suggested, our algorithm is an Upper Confidence Bound (UCB) strategy. In order to define our Upper Confidence Bound, we first define the *count* function, the *corrected count* function, and the *corrected average* function in Definition 2.

Definition 2. *Let \mathcal{P}_t be the partition of \mathcal{A} at time t ($t \geq 1$) and let p_t be the Region Selection function associated with \mathcal{P}_t . Let $(a_1, y_1, a_2, y_2, \dots, a_{t'}, y_{t'})$ be the observations received up to time t' ($t' \geq 1$). We define*

1. *the count function $n_{t,t'}^0 : \mathcal{A} \rightarrow \mathbb{Z}$, such that*

$$n_{t,t'}^0(a) = \sum_{i=1}^{t'} \mathbb{1}[a_i \in p_t(a)],$$

and by convention, $n_{t,0}^0(a) = 0$;

¹PartitionUCB and Contextual PartitionUCB can naturally handle sub-Gaussian noise with zero mean.

2. the corrected count function $n_{t,t'} : \mathcal{A} \rightarrow \mathbb{Z}$, such that

$$n_{t,t'}(a) = \max(1, n_{t,t'}^0(a)); \quad (2)$$

3. the corrected average function $m_{t,t'} : \mathcal{A} \rightarrow \mathbb{R}$, such that

$$m_{t,t'}(a) = \begin{cases} \frac{\sum_{i=1}^{t'} y_i \mathbb{1}_{[a_i \in p_t(a)]}}{n_{t,t'}^0(a)}, & \text{if } n_{t,t'}^0(a) > 0; \\ 1, & \text{otherwise.} \end{cases} \quad (3)$$

In words, $n_{t,t'}^0(a)$ is the number of points among $(a_1, a_2, \dots, a_{t'})$ that are in the same region as arm a , with regions defined by \mathcal{P}_t . It is important to note that the domain of the function $n_{t,t'}^0$ is the arm space \mathcal{A} – although when computing $n_{t,t'}^0(a)$ with $a \in \mathcal{A}$, we need to locate the region that contains a first (using the *region selection* function), the function $n_{t,t'}^0$ always takes an arm $a \in \mathcal{A}$ as input. The functions $n_{t,t'}$ and $m_{t,t'}$ are defined in a similar fashion – all are defined over the arm space \mathcal{A} , with respect to the partition \mathcal{P}_t and the data $(a_1, y_1, \dots, a_{t'}, y_{t'})$. When $t = t'$, we simplify the notations $n_{t,t'}^0$ to n_t^0 , $n_{t,t'}$ to n_t , and $m_{t,t'}$ to m_t . We also denote by $D(\mathcal{S})$ the diameter of $\mathcal{S} \subset \mathcal{A}$, and $D(\mathcal{S}) := \sup_{a, a' \in \mathcal{S}} \|a - a'\|_\infty$.

At time t , based on the partition \mathcal{P}_{t-1} and observations $(a_1, y_1, a_2, y_2, \dots, a_{t-1}, y_{t-1})$, our bandit algorithm use

$$U_t(a) = m_{t-1}(a) + \beta_t \sqrt{\frac{1}{n_{t-1}(a)}}, \quad a \in \mathcal{A} \quad (4)$$

for some β_t ($\beta_t = \Theta(\sqrt{\log t})$) as the Upper Confidence Bound of arm a ; and we play an arm with the highest U_t value (with ties broken uniformly at random).

Since U_t is a piece-wise constant function in the arm space and is constant within each region, playing an arm with the highest U_t with random tie-breaking is equivalent to selecting the best region (under UCB) and randomly select an arm within the region. This strategy (4) takes a similar form to the classic UCB1 algorithm Auer et al. (2002). After we decide which arm to play we update the partition into a finer one if necessary. This strategy, PartitionUCB, is summarized in Algorithm 1.

In order for the algorithm to be well-behaved, i.e., having $R_T = \tilde{O}(T^{\frac{d+1}{d+2}})$, we need the partitions \mathcal{P}_t to follow some regularization conditions. One regularization condition is defined in Definition 3.

Definition 3 (Legal Partition). *For a set of points $\{a_1, a_2, \dots, a_t\} \subset \mathcal{A}$, a partition at time $t \geq 1$ $\mathcal{P}_t = \{P_t^{(1)}, \dots, P_t^{(k_t)}\}$ of $\mathcal{A} \subset \mathbb{R}^d$ is said to be an (α, l) -legal partition (with $\alpha > 0$ and $l > 0$) with respect to $\{a_1, a_2, \dots, a_t\}$ if for all $a \in \mathcal{A}$*

$$l(t+1)^{-\frac{1}{d+2}} \leq D(p_t(a)) \leq l(t+1)^{-\frac{1}{d+2}} + \frac{\alpha}{\sqrt{n_t(a)}},$$

where p_t is defined with respect to \mathcal{P}_t , and n_t is defined with respect to \mathcal{P}_t and $\{a_1, a_2, \dots, a_t\}$.

In addition, we require that for any two partitions \mathcal{P}_t and \mathcal{P}_{t+1} consecutive in time, for any $P^{(i)} \in \mathcal{P}_{t+1}$, there exists $P^{(j)} \in \mathcal{P}_t$ such that $P^{(i)} \subset P^{(j)}$. In words, at round t , some regions of the partition are split into multiple regions to form the partition at round $t+1$. We say that the partition *grows finer*. Practical versions of Algorithm 1 are discussed in Section 3. A high probability regret bound of Algorithm 1 is stated in Theorem 1.

Theorem 1. *Suppose that the payoff function f defined on a compact domain $\mathcal{A} \subset \mathbb{R}^d$ satisfies $f(a) \in [0, 1]$ for all a and is Lipschitz. Then for any given $T \geq 2$, with probability at least $1 - \frac{1}{3\lfloor \sqrt{T} \rfloor^3} + \frac{1}{3T^3}$, the cumulative regret of Algorithm 1 satisfies $R_T = \tilde{O}\left(T^{\frac{d+1}{d+2}}\right)$.*

In order to prove Theorem 1, we first need Lemmas 1, 2 and 3. Lemma 1 is a consequence of the Hoeffding's inequality and the Lipschitzness of the payoff function. Lemma 2 states that the regret at time t can be bounded in terms of the inverse of the squared-root corrected count and the size of the regions in the legal partition with high probability. Lemma 3 is an extension of Lemma 2 and it bounds the cumulative regret R_T by the inverse of the squared-root corrected count.

Algorithm 1 PartitionUCB

1: Inputs: $s > 0$, $c > 0$, $\alpha > 0$, $l > 0$, and the initial partition $\mathcal{P}_0 = \{\mathcal{A}\}$.
2: \triangleright /* s - upper bound of variance of the noise.*/
3: \triangleright /* c - upper bound of the Lipschitz constant.*/
4: \triangleright /* α and l - legal partition parameters.*/
5: **for** $t = 1, 2, \dots$ **do**
6: With respect to \mathcal{P}_{t-1} and past observations up to time $t-1$, define m_{t-1} and n_{t-1} as in (3) and (2). Play
$$a_t \in \arg \max_{a \in \mathcal{A}} \left\{ m_{t-1}(a) + \beta_t \sqrt{\frac{1}{n_{t-1}(a)}} \right\}$$

 with $\beta_t = \alpha c + \sqrt{\left(\frac{1}{2} + 2s^2\right) (4 \log t + \log 2)}$. Ties are broken uniformly at random.
7: Observe payoff y_t associated with a_t .
8: Update the partition \mathcal{P}_{t-1} into \mathcal{P}_t so that the partition grows finer and is an (α, l) -legal partition.

Lemma 1. *Let n_t and m_t be the corrected count and the corrected average defined with respect to the legal partition \mathcal{P}_t and observations $(a_1, y_1, a_2, y_2, \dots, a_t, y_t)$. At any time $t \geq 1$, with probability greater than or equal to $1 - \frac{1}{t^4}$,*

$$|f(a) - m_{t-1}(a)| \leq clt^{-\frac{1}{d+2}} + \sqrt{\frac{1}{n_{t-1}(a)}}\alpha c + \sqrt{\left(\frac{1}{2} + 2s^2\right) (4 \log t + \log 2)} \quad (5)$$

where s is the standard deviation of the Gaussian noise in the observation, c is the Lipschitz constant, d is the dimension of the arm space, and α and l define the legal partition.

Lemma 2. *Let n_t be the corrected count defined with respect to the legal partition \mathcal{P}_t and observations up to time t $(a_1, y_1, a_2, y_2, \dots, a_t, y_t)$. At any time $t \geq 1$, with probability greater than or equal to $1 - \frac{1}{t^4}$, the regret r_t satisfies*

$$r_t \leq 2 \left(\frac{\beta_t}{\sqrt{n_{t-1}(a_t)}} + clt^{-\frac{1}{d+2}} \right) \quad (6)$$

where $\beta_t = \alpha c + \sqrt{\left(\frac{1}{2} + 2s^2\right) (4 \log t + \log 2)}$.

Lemma 3. *Let n_t be the corrected count defined with respect to the legal partition \mathcal{P}_t and observations up to time t $(a_1, y_1, a_2, y_2, \dots, a_t, y_t)$. For $T \geq 2$, with probability at least $1 - \frac{1}{3\lfloor \sqrt{T} \rfloor^3} + \frac{1}{3T^3}$, the cumulative regret R_T satisfies*

$$R_T \leq 2\beta_T \sum_{t=\lfloor \sqrt{T} \rfloor + 1}^T \frac{1}{\sqrt{n_{t-1}(a_t)}} + \mathcal{O}(T^{\frac{d+1}{d+2}}). \quad (7)$$

To prove Theorem 1, it remains to bound

$$\sum_{t=\lfloor \sqrt{T} \rfloor + 1}^T \frac{1}{\sqrt{n_{t-1}(a_t)}}. \quad (8)$$

For any $a \in \mathcal{A}$, $n_t(a)$ is not necessarily increasing with t , since the partition grows finer. This results in difficulty in bounding (8). Next, we present a constructive trick to bound (8). For each T , we can construct a hypothetical noisy degenerate Gaussian process to bound (8). We are not assuming our payoffs are drawn from these Gaussian processes. We only use the construction to bound (8). To construct these noisy degenerate Gaussian processes, we define the kernel functions $k_T : \mathcal{A} \times \mathcal{A} \rightarrow \mathbb{R}$,

$$k_T(a, a') = \begin{cases} 1, & \text{if } p_T(a) = p_T(a') \\ 0, & \text{otherwise.} \end{cases} \quad (9)$$

where p_T is the region selection function defined with respect to \mathcal{P}_T . The kernel k_T is positive semi-definite as shown in Proposition 1.

Proposition 1. *The kernel defined in (9) is positive semi-definite for any $T \geq 1$.*

Proof. For any x_1, \dots, x_n in where the kernel $k_T(\cdot, \cdot)$ is defined, the Gram matrix $K = [k_T(x_i, x_j)]_{n \times n}$ can be written into block diagonal form where diagonal blocks are all-one matrices and off-diagonal blocks are all zeros with proper permutations of rows and columns. Thus without loss of generality, for any vector $\mathbf{v} = [v_1, v_2, \dots, v_n] \in \mathbb{R}^n$, $\mathbf{v}^\top K \mathbf{v} = \sum_{b=1}^B \left(\sum_{j: i_j \text{ in block } b} v_{i_j} \right)^2 \geq 0$ where the first summation is taken over all diagonal blocks and B is the total number of diagonal blocks in the Gram matrix. \square

Now, at any time T , let us consider the model $\tilde{y}(a) = g(a) + e$ where g is drawn from a Gaussian process $g \sim \mathcal{GP}(0, k_T(\cdot, \cdot))$ and $e_T \sim \mathcal{N}(0, s_T^2)$. Suppose that the arms and hypothetical payoffs $(a_1, \tilde{y}_1, a_2, \tilde{y}_2, \dots, a_t, \tilde{y}_t)$ are observed from this Gaussian process. The posterior variance for this Gaussian process after the observations at a_1, a_2, \dots, a_t is

$$\sigma_{T,t}^2(a) = k_T(a, a) - \mathbf{k}^\top (K + s_T^2 I)^{-1} \mathbf{k}$$

where $\mathbf{k} = [k_T(a, a_1), \dots, k_T(a, a_t)]^\top$, $K = [k_T(a_i, a_j)]_{t \times t}$ and I is the identity matrix. In other words, $\sigma_{T,t}^2(a)$ is the posterior variance using points up to time t with the kernel defined by the partition at time T . After some matrix manipulation, we know that

$$\sigma_{T,t}^2(a) = 1 - \mathbf{1}[\mathbf{1}\mathbf{1}^\top + s_T^2 I]^{-1} \mathbf{1},$$

where $\mathbf{1} = [1, \dots, 1]_{1 \times n_{T,t}^0(a)}^\top$. By the Sherman-Morrison formula, $[\mathbf{1}\mathbf{1}^\top + s_T^2 I]^{-1} = s_T^{-2} I - \frac{s_T^{-4} \mathbf{1}\mathbf{1}^\top}{1 + s_T^{-2} n_{T,t}^0(a)}$. Thus the posterior variance is $\sigma_{T,t}^2(a) = \frac{1}{1 + s_T^{-2} n_{T,t}^0(a)}$. Now, we can link the sum of variances in the constructed Gaussian processes to (8), since the posterior variances $\sigma_{T,t}^2(a)$ in these Gaussian processes can be used to bound the term $\frac{1}{\sqrt{n_{t-1}(a)}}$. Lemma 4 bounds the sum of posterior variances in the constructed Gaussian process in terms of the cardinality of the partition $|\mathcal{P}_T|$. Lemma 5 bounds (8) using the fact that $\frac{1}{n_{t-1}(a_t)} \leq (1 + s_T^{-2}) \sigma_{T,t-1}^2(a_t)$ (See Appendix A.5) and Lemma 4. Therefore, the constructed Gaussian processes bridge (8) and the cardinality of the partition $|\mathcal{P}_t|$. When the partition \mathcal{P}_t is a Legal Partition, we can bound its cardinality. This sketches a proof for Lemma 5. Lemmas 3 and 5 lead directly to a proof for Theorem 1, since all terms in (7) are $\tilde{\mathcal{O}}(T^{\frac{d+1}{d+2}})$.

Lemma 4. *For data generated from the noisy Gaussian process $g \sim \mathcal{GP}(0, k_T(\cdot, \cdot))$ and $\tilde{y} = g + e$ with $e \sim \mathcal{N}(0, s_T^2)$, if we query at points $\mathbf{a}_t = (a_1, \dots, a_t)$, then*

$$\sum_{\tau=1}^t \log(1 + s_T^{-2} \sigma_{T,\tau-1}^2(a_\tau)) \leq |\mathcal{P}_T| \log\left(1 + \frac{s_T^{-2} t}{|\mathcal{P}_T|}\right) \quad (10)$$

where $\sigma_{T,\tau-1}^2(a_\tau) = \frac{1}{1 + s_T^{-2} n_{T,\tau-1}^0(a_\tau)}$ and $|\mathcal{P}_T|$ is the cardinality of the partition associated with $k_T(\cdot, \cdot)$.

Lemma 5. *For $T \geq 2$,*

$$\sum_{t=\lfloor \sqrt{T} \rfloor + 1}^T \sqrt{\frac{1}{n_{t-1}(a_t)}} = \mathcal{O}(T^{\frac{d+1}{d+2}}). \quad (11)$$

Detailed proofs of all lemmas are in Appendix A.

2.2 The Contextual PartitionUCB algorithm

In this section, we present an extension of Algorithm 1 for the contextual stochastic bandit problem. The contextual stochastic bandit problem is an extension to the stochastic bandit problem. In this problem, at each time, context information is revealed, and the agent chooses an arm based on past experience as well as the contextual information. Formally, the payoff function f is defined over the product of the context space \mathcal{Z} and the arm space \mathcal{A} and takes values from $[0, 1]$. Similar to the previous discussions, compactness of the product space and Lipschitzness of the payoff function are assumed. At each time t , a contextual vector $z_t \in \mathcal{Z}$ is revealed and the agent plays an arm $a_t \in \mathcal{A}$. The performance of the agent is measured by the cumulative contextual regret

$$R_T^c = \sum_{t=1}^T f(z_t, a_t^*) - f(z_t, a_t), \quad (12)$$

where $f(z_t, a_t^*)$ is the maximal value of f given contextual information z_t . Here, a_t^* is the maximizer of $f(z_t, \cdot)$. Surprisingly, a simple extension of Algorithm 1 can solve the contextual version problem. In the contextual case, we partition the joint space $\mathcal{Z} \times \mathcal{A}$ instead of the arm space \mathcal{A} . As an analog to (2) and (3), we define the corrected count n_t and the corrected average m_t over the joint space $\mathcal{Z} \times \mathcal{A}$ with respect to the partition \mathcal{P}_t of the joint space $\mathcal{Z} \times \mathcal{A}$, and observations in the joint space $((z_1, a_1), y_1, \dots, (z_t, a_t), y_t)$.

Algorithm 2 Contextual PartitionUCB

```

1: Inputs:  $s > 0, c > 0, \alpha > 0, l > 0$ , and the initial partition  $\mathcal{P}_0 = \{\mathcal{Z} \times \mathcal{A}\}$ .
2:                                     ▷ /*  $s$  - upper bound of variance of the noise.*/
3:                                     ▷ /*  $c$  - upper bound of the Lipschitz constant.*/
4:                                     ▷ /*  $\alpha$  and  $l$  - legal partition parameter.*/
5:
6: for  $t = 1, 2, \dots$  do
7:   Observe  $z_t \in \mathcal{Z}$ .
8:   With respect to the partition  $\mathcal{P}_{t-1}$  and observations up to time  $t - 1$ , define  $m_{t-1}$  and  $n_{t-1}$  as in (3) and (2) (but on the
   joint space  $\mathcal{Z} \times \mathcal{A}$ ). Play
                                     
$$a_t \in \arg \max_{a \in \mathcal{A}} \left\{ m_{t-1}(z_t, a) + \beta_t \sqrt{\frac{1}{n_{t-1}(z_t, a)}} \right\}$$

   with  $\beta_t = \alpha c + \sqrt{\left(\frac{1}{2} + 2s^2\right)(4 \log t + \log 2)}$ . Ties are broken uniformly at random.
9:   Observe payoff  $y_t$  associated with  $(z_t, a_t)$ .
10:  Update the partition  $\mathcal{P}_{t-1}$  into  $\mathcal{P}_t$  so that the partition grows finer and is an  $(\alpha, l)$ -legal partition of  $\mathcal{Z} \times \mathcal{A}$ .

```

The regret bound of Algorithm 2 is in Corollary 1.

Corollary 1. *Suppose that the payoff function f defined on a compact domain $\mathcal{Z} \times \mathcal{A} \subset \mathbb{R}^d$ satisfies $f(z, a) \in [0, 1]$ for all (z, a) and is Lipschitz. Then for any given $T \geq 2$, with probability at least $1 - \frac{1}{3\lfloor \sqrt{T} \rfloor^3} + \frac{1}{3T^3}$, the cumulative contextual regret of Algorithm 2 satisfies $R_T^c = \tilde{O}\left(T^{\frac{d+1}{d+2}}\right)$.*

Corollary 1 is an extension of Theorem 1. Since Lemmas 4 and 5 holds for any sequence of (context-)arms, we can replace regret with contextual regret and slightly alter Lemmas 1, 2 and 3 to prove Corollary 1.

3 Implementation and Experiments

3.1 Regression Tree Implementation

One nice property of Algorithm 1 is that it does not impose constraints on how to construct the partition. Therefore we can use a greedy criterion for constructing regression trees to construct the partition. Leaves in a regression tree form a partition of the space in the sense that (1) is satisfied. At the same time, a regression tree is designed to fit the underlying function. This property tends to result in an adaptive partition where the underlying function values within each region are relatively close to each other. For this paper, we use the *Mean Absolute Error (MAE)* reduction criterion Breiman et al. (1984) to adaptively construct a regression tree. More specifically, a node \mathbf{N} containing data samples $\{(a_1, y(a_1)), (a_2, y(a_2)), \dots, (a_n, y(a_n))\}$ is split along a feature (can be randomly selected for scalability) into \mathbf{N}_1 and \mathbf{N}_2 (where $\mathbf{N}_1 \cup \mathbf{N}_2 = \mathbf{N}$ and $\mathbf{N}_1 \cap \mathbf{N}_2 = \emptyset$) such that the following reduction in MAE is maximized:

$$MAE(\mathbf{N}) - \left(\frac{|\mathbf{N}_1|}{|\mathbf{N}|} MAE(\mathbf{N}_1) + \frac{|\mathbf{N}_2|}{|\mathbf{N}|} MAE(\mathbf{N}_2) \right) \quad (13)$$

where $MAE(\mathbf{N}) = \frac{1}{|\mathbf{N}|} \sum_{a_i \in \mathbf{N}} |y(a_i) - \hat{y}(\mathbf{N})|$ and $\hat{y}(\mathbf{N}) = \frac{1}{|\mathbf{N}|} \sum_{a_i \in \mathbf{N}} y(a_i)$. The nodes are recursively split until the maximal possible reduction in *MAE* is smaller than η . The leaves are then used to form a partition. Each region is again associated with a corrected mean and corrected count. Using regression trees, we develop the TreeUCB algorithm (TUCB), and the Contextual TreeUCB algorithm (CTUCB), as summarized in Algorithms 3 and 4. Although tree implementation may result in partitions that are not legal, the empirical results show that in practice the heuristic developed based on the regression tree implementation outperforms most state-of-the-art in tuning neural networks as we will see in Section 3.2. The coding of TUCB and CTUCB is based on a modified `scikit-learn` package Pedregosa et al. (2011).

3.2 Application to Neural Network tuning

Experimental design: Given fixed training and validation sets, the validation accuracy of a neural network can be viewed as a noisy function of hyperparameters. Typical hyperparameters for tuning include the network

Algorithm 3 TreeUCB (TUCB)

- 1: Parameter: $\beta_t \geq 0, \eta > 0$. \triangleright /* $\beta_t = \Theta(\sqrt{\log t})$ trades off exploration and exploitation. η is the minimal allowed gain in MAE when fitting a regression tree. */
- 2: **for** $t = 1, 2, \dots, N$ **do**
- 3: Fit a regression tree f_{t-1} (using (13)) on observations $(a_1, y_1, a_2, y_2, \dots, a_{t-1}, y_{t-1})$, stop growing the tree if the gain in MAE is smaller than η .
- 4: With respect to the partition \mathcal{P}_{t-1} defined by leaves of f_{t-1} , define n_{t-1}, m_{t-1} as in (2) and (3). Play

$$a_t \in \arg \max_{a \in \mathcal{A}} \left\{ m_{t-1}(a) + \beta_t \sqrt{\frac{1}{n_{t-1}(a)}} \right\}.$$

Ties are broken uniformly at random.

- 5: Observe the reward y_t .
-

Algorithm 4 Contextual TreeUCB (CTUCB)

- 1: Parameter: $\beta_t \geq 0, \eta > 0$. \triangleright /* $\beta_t = \Theta(\sqrt{\log t})$ trades off exploration and exploitation. η is the minimal allowed gain in MAE when fitting a regression tree. */
- 2: **for** $t = 1, 2, \dots, N$ **do**
- 3: Observe context z_t .
- 4: Fit a regression tree f_{t-1} (using (13)) on observations $((z_1, a_1), y_1, (z_2, a_2), y_2, \dots, (z_{t-1}, a_{t-1}), y_{t-1})$, stop growing the tree if the gain in MAE is smaller than η .
- 5: With respect to the partition \mathcal{P}_{t-1} defined by leaves of f_{t-1} , define n_{t-1} and m_{t-1} in (2) and (3) (but over the joint space $\mathcal{Z} \times \mathcal{A}$). Play

$$a_t \in \arg \max_{a \in \mathcal{A}} \left[m_{t-1}(z_t, a) + \beta_t \sqrt{\frac{1}{n_{t-1}(z_t, a)}} \right].$$

Ties are broken uniformly at random.

- 6: Observe the reward y_t .
-

architecture, learning rate, training iterations, etc. The number of training iterations is itself a hyperparameter, but it is a special one – training accuracy tends to increase with the number of training iterations, and we may only care about the performance at a large enough training iteration. In addition, some tuning methods have a special scheme to leverage the training iterations as a special dimension, while some do not. Therefore we divide the experiments into two settings: A) the algorithms are agnostic to the training resource and thus tune the training iterations together with all other hyperparameters; B) the algorithms leverage the number of training iterations as a special dimension using their own schemes (if it has one). We will refer to these two settings as *setting A* and *setting B* from now on; we compare TUCB against other methods in Setting A, and compare CTUCB against other methods in Setting B.

Using training iterations as contextual information. Context is usually observed from the environment, but in this case, we are able to choose it. We let CTUCB start with a small number of training iterations and progressively increase the number of iterations. By doing this, CTUCB can use information obtained at smaller iterations (cheaper to obtain) to help infer the performance at larger iterations (more expensive to obtain). This assumes that a configuration that is good at smaller iterations tends to be good at larger iterations as well, which tended to be true in practice for our experiments. As shown in Figures 1, 2 and 3 by using training iterations as the contextual information, CTUCB can outperform existing state-of-the-art methods.

Modeling the Lipschitz constant with the number of training iterations. In *setting B*, for a hyperparameter configuration a , as the training iteration z increases, the validation accuracy converges. Therefore, on a local scale, the Lipschitz constant decreases as the training iteration (epoch) increases. As stated in Algorithm 2, the confidence coefficient is $\beta_t \sqrt{\frac{1}{n_{t-1}(z, a)}}$ with $\beta_t = \alpha c + \sqrt{(\frac{1}{2} + 2s^2)(4 \log t + \log 2)}$. Instead of using the global Lipschitz constant c , we can use $\mathcal{C}(z)$ to model the local Lipschitz constant if there is enough prior knowledge. Since neural networks converge as training resource increases, $\mathcal{C}(z)$ should be positive and decreases with z .

3.3 Experiments

In this section, we compare the performance of TUCB and CTUCB on the MNIST dataset, the SVHN dataset, and the CIFAR-10 dataset. In *setting A* we compare SMAC, random search, TPE, Spearmint, Harmonica (Harmonica using random search as the base algorithm) and TUCB. In *setting B*, we compare SMAC, random search, TPE, Spearmint, CTUCB, Hyperband and Harmonica-h (Harmonica using Hyperband as the base algorithm). In *setting B*, CTUCB, Hyperband and Harmonica-h set the *number of training iterations* using

their own schemes, while the rest of the algorithms fix the *number of training iterations* and tune the rest of the hyperparameters. In particular, CTUCB uses the number of training iterations as the contextual information. How we set the training iterations for CTUCB will be specified later.

3.3.1 MLP for MNIST

In this section, we tune a simple Multi-Layer Perceptron (MLP) and compare TUCB and CTUCB with state-of-the-art methods. For TUCB, we use $\beta_t = v\sqrt{\log t}$, where v is a hyperparameter of the tuning algorithm; and for CTUCB in tuning neural networks, we use $\beta_t = v_1\sqrt{\log t} + v_2z^{v_3}$, where z is the number of training iterations, and $v_2z^{v_3}$ models the local Lipschitz constant. In this case, v_1, v_2 and v_3 are all hyperparameters of the tuning algorithm. Although TUCB and CTUCB have their own hyperparameters, the performance of both TUCB and CTUCB are not sensitive to these hyperparameters. The architecture of this MLP is as follows: in the feed-forward direction, there are the *input layer*, the *fully connected hidden layer with dropout ensemble*, and then the *output layer*. The hyperparameter search space is *number of hidden neurons* (range $[10, 784]$), *learning rate* ($[0.0001, 4)$), *dropout rate* ($[0.1, 0.9)$), *batch size* ($[10, 500]$), *number of iterations* ($[30, 243]$). In *setting B*: All algorithms except for Hyperband, CTUCB, Harmonica-h always use 243 for the number of iterations.² Hyperband, CTUCB and Harmonica-h use their own specific mechanisms to alter *number of iterations*. The results are shown in Figure 1. For CTUCB in Setting B, we choose the training iterations z_t so that

$$z_t = \begin{cases} \lfloor 1/(1/30 - (t \bmod 33)(1/30 - 1/243)/29) \rfloor, \\ \quad \text{if } t \bmod 33 < 30, \\ 243, \quad \text{otherwise.} \end{cases}$$

By setting z_t this way, CTUCB repeatedly starts with small iterations and proceeds to larger iterations (and repeats). As shown in Figure 1, our methods find good configurations faster than other methods, in both Setting A and Setting B.

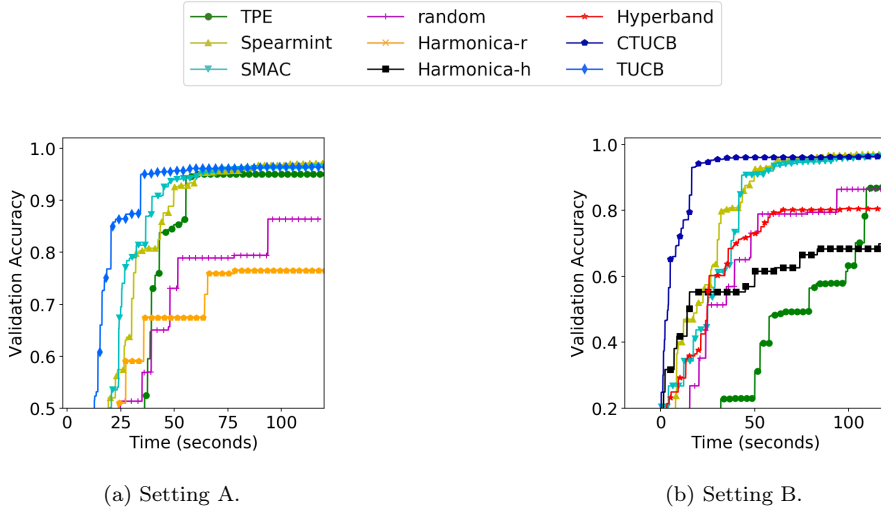


Figure 1: Current best validation accuracy against wall clock time on MNIST. *Left*: Setting A. TUCB: $v = 0.1, \eta = 0.0001$. *Right*: Setting B. CTUCB: $v_1 = 0.1, v_2 = 1, v_3 = -2, \eta = 0.0001$. The results for all methods are averaged over 10 runs. As is shown in the plots, TUCB and CTUCB find good configurations faster than other methods for the experiments in Section 3.3.1.

3.4 AlexNet CNN for SVHN

In this section, we tune an AlexNet-type Krizhevsky et al. (2012) CNN LeCun et al. (1998) for the SVHN dataset and compare TUCB and CTUCB with state-of-the-art methods. The architecture of this CNN and the corresponding hyperparameters are summarized in Table 1a and 1b. The results are shown below in Figure 2.

²We choose the number 243 so that it helps Hyperband avoid rounding using their example down-sampling rate 3.

For CTUCB in Setting B, we pick context z_t (the training iterations) so that

$$z_t = \begin{cases} \lfloor 1/(1/100 - (t \bmod 34)(1/100 - 1/1500)/29) \rfloor, & \text{if } t \bmod 34 < 30, \\ 1500, & \text{otherwise.} \end{cases}$$

By setting z_t in this way, CTUCB starts with small training iteration and progressively increases it (and repeats). In this set of experiments, TUCB and CTUCB usually find good configurations at least as fast as other methods.

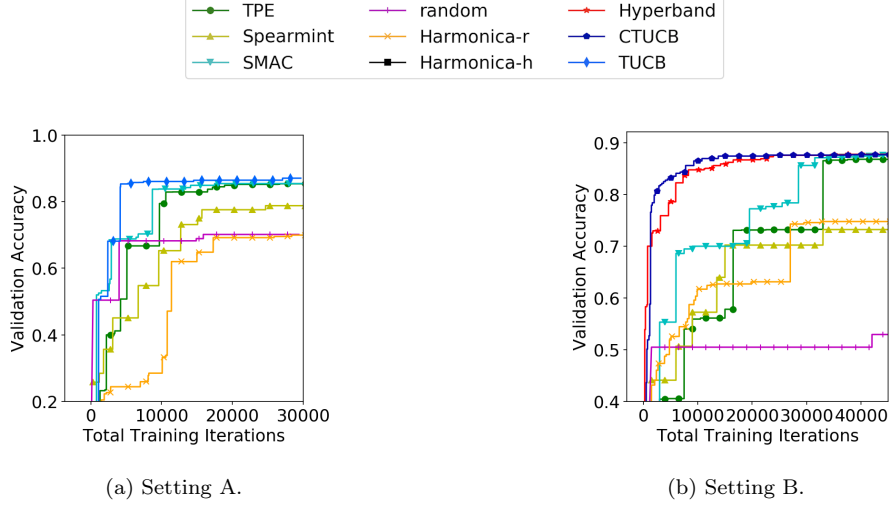


Figure 2: Current best validation accuracy against total training iterations used on SVHN. *Left:* Setting A. TUCB: $v_1 = 0.1, \eta = 0.001$. *Right:* Setting B. CTUCB: $v_1 = 0.1, v_2 = 1, v_3 = -2, \eta = 0.001$. All other algorithms use default setting. The results for all methods are averaged over 5 runs. For all methods, if a configuration diverged (having a diverging cross-entropy loss), its chosen number of iterations is used as the training resource used, even if the training terminates early because of the diverging cost.

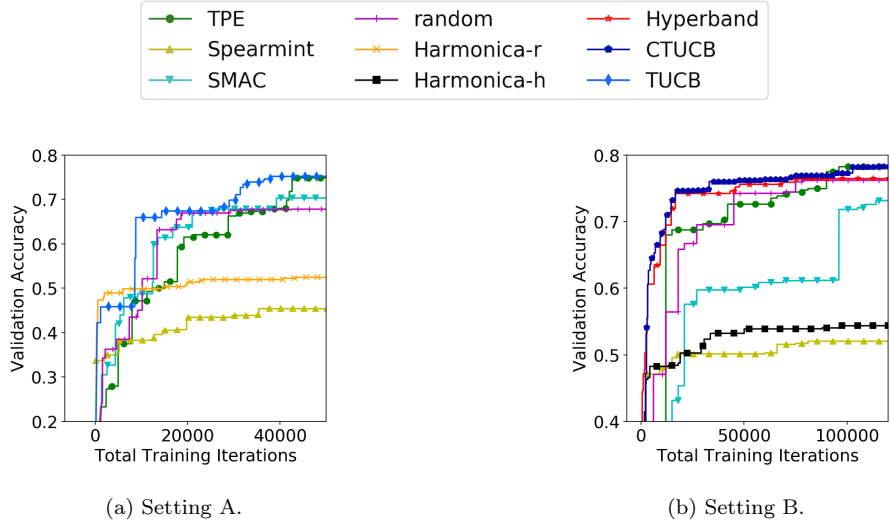


Figure 3: Plot of current best validation accuracy versus total training iterations used on CIFAR. *Left:* Setting A. TUCB: $v_1 = 0.1, \eta = 0.0001$. *Right:* Setting B. CTUCB: $v_1 = 0.1, v_2 = 1, v_3 = -2, \eta = 0.0001$. All other algorithms use default setting. The results for all methods are averaged over 5 runs. As is shown in the plots, TUCB and CTUCB find good configurations faster than other methods most of the time. In Setting A, Harmonica performed slightly better in early stage, but TUCB achieves a higher final accuracy. In Setting B, Hyperband ties CTUCB and both Hyperband and CTUCB are better than other methods. For all methods, if a configuration diverged (having a diverging cross-entropy loss), its chosen number of iterations is still used as the training resource used. For all methods, if a configuration diverged (having a diverging cross-entropy loss), its chosen number of iterations is used as the training resource used, even if the training terminates early because of the diverging cost.

Layer	Hyperparameters	values
Conv1	conv1-kernel-size	*
	conv1-number-of-channels	200
	conv1-stride-size	(1,1)
	conv1-padding	"same"
MaxPooling1	pooling1-size	(3,3)
	pooling1-stride	(1,1)
	pooling1-padding	"same"
Conv2	conv2-kernel-size	*
	conv2-number-of-channels	200
	conv2-stride-size	(1,1)
	conv2-padding	"same"
MaxPooling2	pooling2-size	(3,3)
	pooling2-stride	(2,2)
	pooling2-padding	"same"
Conv3	conv3-kernel-size	(3,3)
	conv3-number-of-channels	200
	conv3-stride-size	(1,1)
	conv3-padding	"same"
AvgPooling3	pooling3-size	(3,3)
	pooling3-stride	(1,1)
	pooling3-padding	"same"
Dense	batch-normalization	default
	number-of-hidden-units	512
	dropout-rate	0.5

(a) CNN architecture for SVHN. A value with * means that this parameter is tuned, and the batch-normalization layer uses all Tensorflow’s default setting.

Hyperparameters	Range
conv1-kernel-size	$\{1, 2, \dots, 7\}$
conv2-kernel-size	$\{1, 2, \dots, 7\}$
β_1	$\{0, 0.05, \dots, 1\}$
β_2	$\{0, 0.05, \dots, 1\}$
learning-rate	1e-6 to 5
training-iteration (only for Setting A)	$\{300, 400, \dots, 1500\}$

(b) Hyperparameter search space. β_1 and β_2 are parameters for the Adamoptimizer. The learning rate is discretized in the following way: from 1e-6 to 1 (including the end points), we log-space the learning rate into 50 points, and from 1.08 to 5 (including the end points) we linear-space the learning rate into 49 points.

Table 1: Settings for the SVHN experiments.

3.4.1 AlexNet CNN for CIFAR-10

In this section, we tune an AlexNet-type Krizhevsky et al. (2012) CNN LeCun et al. (1998) for the CIFAR-10 dataset Krizhevsky and Hinton (2009) and compare TUCB and CTUCB with state-of-the-art methods. The architecture of this CNN and the corresponding hyperparameters are summarized in Table 2a and 2b. The results are shown below in Figure 3. For CTUCB in Setting B, we pick context z_t (the training iterations) so that CTUCB increases the number of training iterations in exactly the same way as Hyperband. Hyperband and CTUCB increase the number of training as shown in Table 3. This progression of training iterations is determined by Hyperband’s hyperparameters. Please refer to the Hyperband paper Li et al. (2016) for more details on how Hyperband selects training resources.

Layer	Hyperparameters	values
Conv1	conv1-kernel-size	*
	conv1-number-of-channels	200
	conv1-stride-size	(1,1)
	conv1-padding	“same”
MaxPooling1	pooling1-size	*
	pooling1-stride	(1,1)
	pooling1-padding	“same”
Conv2	conv2-kernel-size	*
	conv2-number-of-channels	200
	conv2-stride-size	(1,1)
	conv2-padding	“same”
MaxPooling2	pooling2-size	*
	pooling2-stride	(2,2)
	pooling2-padding	“same”
Conv3	conv3-kernel-size	*
	conv3-number-of-channels	200
	conv3-stride-size	(1,1)
	conv3-padding	“same”
AvgPooling3	pooling3-size	*
	pooling3-stride	(1,1)
	pooling3-padding	“same”
Dense	batch-normalization	default
	number-of-hidden-units	512
	dropout-rate	0.5

(a) CNN architecture for CIFAR-10. A value with * means that this parameter is tuned, and the batch-normalization layer uses all Tensorflow’s default setting.

Hyperparameters	Range
conv1-kernel-size	$\{1, 2, \dots, 7\}$
conv2-kernel-size	$\{1, 2, \dots, 7\}$
conv3-kernel-size	$\{1, 2, 3\}$
pooling1-size	$\{1, 2, 3\}$
pooling2-size	$\{1, 2, 3\}$
pooling3-size	$\{1, 2, \dots, 6\}$
β_1 & β_2	$\{0, 0.05, \dots, 1\}$
learning-rate	1e-6 to 5
learning-rate-reduction	$\{1, 2, 3\}$
training-iteration (only for Setting A)	$\{200, 400, \dots, 3000\}$

(b) Hyperparameter search space. β_1 and β_2 are parameters for the Adamoptimizer. The learning rate is discretized in the following way: from 1e-6 to 1 (including the end points), we log-space the learning rate into 50 points, and from 1.08 to 5 (including the end points) we linear-space the learning rate into 49 points. The learning-rate-reduction parameter is how many times the learning rate is going to be reduced by a factor of 10. For example, if the total training iteration is 200, the learning-rate is 1e-6, and the learning-rate-reduction is 1, then for the first 100 iteration the learning rate is 1e-6, and the for last 100 iterations the learning rate is 1e-7.

Table 2: Settings for CIFAR-10 experiments.

Training Iterations	Number of different configurations
263	12
395	8
592	5
888	3
1333	2
2000	1
3000	1
395	8
592	5
888	3
1333	2
2000	1
3000	1
592	6
888	4
1333	2
2000	1
3000	1
888	4
1333	2
2000	1
3000	1
1333	5
2000	3
3000	2
2000	5
3000	3
3000	7

Table 3: The pattern of resource increase for Hyperband and CTUCB in Section 3.4.1. The table represents the resource increase in the following way. The first row states that Hyperband and CTUCB first train 12 different neural networks, each with 263 training iterations; then the second row states that both algorithms then train 8 neural network each with 395 iterations; and so on.

As shown in Figure 3, our methods find good configurations faster than other methods most of the time. In particular, in Setting A, TUCB reaches 70% accuracy using 30,400 iterations, while other methods on average require 42,800 iterations; in Setting B, TUCB reaches 70% accuracy using 11,943 iterations, while other methods on average require 71,934 total iterations.³ In addition, TUCB does not achieve above 0.754 accuracy after 45,000 iterations in Setting A, while CTUCB achieves above 0.76 accuracy within 45,000 iterations in Setting B. This shows that leveraging the training iterations as a special dimension can help increase the accuracy on an absolute scale.

4 Conclusion

We propose the PartitionUCB and the Contextual PartitionUCB algorithms that successively partition the arm space and the context-arm space and play the Upper Confidence Bound strategy based on the partition. We also provide high probability regret upper bounds for both algorithms. Since a decision tree corresponds to a partition of the space, fast implementations using regression trees called TUCB and CTUCB are provided. Empirical studies show that TUCB and CTUCB are competitive with the state-of-the-art methods for tuning neural networks, and could save substantial computing resources. As suggested by the results in the paper, more bandit algorithms could be considered as benchmarks for the problem of neural network tuning.

³In our averages for Setting A, for methods that required over 45,000 iterations to reach 70% accuracy, we simply denoted that they required 45,000 iterations. In our averages for Setting B, for methods that required over 120,000 iterations to reach 70% accuracy, we simply denoted that they required 120,000 iterations.

Acknowledgement

The authors are grateful to Aaron J Fisher, Tiancheng Liu and Weicheng Ye for their comments and insights. The project is partially supported by the Alfred P. Sloan Foundation through the Duke Energy Data Analytics fellowship.

References

- Abbasi-Yadkori, Y., Pál, D., and Szepesvári, C. (2011). Improved algorithms for linear stochastic bandits. In *Advances in Neural Information Processing Systems*, pages 2312–2320.
- Abeille, M., Lazaric, A., et al. (2017). Linear thompson sampling revisited. *Electronic Journal of Statistics*, 11(2):5165–5197.
- Agrawal, R. (1995). Sample mean based index policies by $o(\log n)$ regret for the multi-armed bandit problem. *Advances in Applied Probability*, 27(4):1054–1078.
- Agrawal, S. and Goyal, N. (2012). Analysis of thompson sampling for the multi-armed bandit problem. In *Conference on Learning Theory*, pages 39–1.
- Agrawal, S. and Goyal, N. (2013). Thompson sampling for contextual bandits with linear payoffs. In *International Conference on Machine Learning*, pages 127–135.
- Auer, P. (2002). Using confidence bounds for exploitation-exploration trade-offs. *Journal of Machine Learning Research*, 3(Nov):397–422.
- Auer, P., Cesa-Bianchi, N., and Fischer, P. (2002). Finite-time analysis of the multiarmed bandit problem. *Machine learning*, 47(2-3):235–256.
- Auer, P., Ortner, R., and Szepesvári, C. (2007). Improved rates for the stochastic continuum-armed bandit problem. In *International Conference on Computational Learning Theory*, pages 454–468. Springer.
- Bergstra, J. and Bengio, Y. (2012). Random search for hyper-parameter optimization. *Journal of Machine Learning Research*, 13(Feb):281–305.
- Bergstra, J. S., Bardenet, R., Bengio, Y., and Kégl, B. (2011). Algorithms for hyper-parameter optimization. In *Advances in neural information processing systems*, pages 2546–2554.
- Breiman, L., Friedman, J., Stone, C. J., and Olshen, R. A. (1984). *Classification and regression trees*. CRC press.
- Bubeck, S., Munos, R., Stoltz, G., and Szepesvári, C. (2011). X-armed bandits. *Journal of Machine Learning Research*, 12(May):1655–1695.
- Calandra, R., Seyfarth, A., Peters, J., and Deisenroth, M. P. (2016). Bayesian optimization for learning gaits under uncertainty. *Annals of Mathematics and Artificial Intelligence*, 76(1-2):5–23.
- Chaloner, K. and Verdinelli, I. (1995). Bayesian experimental design: A review. *Statistical Science*, pages 273–304.
- Contal, E., Perchet, V., and Vayatis, N. (2014). Gaussian process optimization with mutual information. In *International Conference on Machine Learning*, pages 253–261.
- Dani, V., Hayes, T. P., and Kakade, S. M. (2008). Stochastic linear optimization under bandit feedback. In *COLT*, pages 355–366.
- de Freitas, N., Smola, A., and Zoghi, M. (2012). Exponential regret bounds for gaussian process bandits with deterministic observations. In *International Conference on Machine Learning (ICML)*.
- Gelbart, M. A., Snoek, J., and Adams, R. P. (2014). Bayesian optimization with unknown constraints. *arXiv preprint arXiv:1403.5607*.
- Geurts, P., Ernst, D., and Wehenkel, L. (2006). Extremely randomized trees. *Machine learning*, 63(1):3–42.

- Gittins, J. C. (1979). Bandit processes and dynamic allocation indices. *Journal of the Royal Statistical Society. Series B (Methodological)*, pages 148–177.
- Hazan, E., Klivans, A., and Yuan, Y. (2017). Hyperparameter optimization: A spectral approach. *arXiv preprint arXiv:1706.00764*.
- Hutter, F., Hoos, H. H., and Leyton-Brown, K. (2011). Sequential model-based optimization for general algorithm configuration. In *International Conference on Learning and Intelligent Optimization*, pages 507–523. Springer.
- Jamieson, K. and Talwalkar, A. (2016). Non-stochastic best arm identification and hyperparameter optimization. In *Artificial Intelligence and Statistics*, pages 240–248.
- Kandasamy, K., Dasarathy, G., Schneider, J., and Póczos, B. (2017). Multi-fidelity bayesian optimisation with continuous approximations. *arXiv preprint arXiv:1703.06240*.
- Kleinberg, R., Slivkins, A., and Upfal, E. (2008). Multi-armed bandits in metric spaces. In *Proceedings of the fortieth annual ACM symposium on Theory of computing*, pages 681–690. ACM.
- Kocsis, L. and Szepesvári, C. (2006). Bandit based monte-carlo planning. In *European conference on machine learning*, pages 282–293. Springer.
- Krizhevsky, A. and Hinton, G. (2009). Learning multiple layers of features from tiny images.
- Krizhevsky, A., Sutskever, I., and Hinton, G. E. (2012). Imagenet classification with deep convolutional neural networks. In *Advances in neural information processing systems*, pages 1097–1105.
- Lai, T. L. and Robbins, H. (1985). Asymptotically efficient adaptive allocation rules. *Advances in applied mathematics*, 6(1):4–22.
- LeCun, Y. (1999). The mnist database of handwritten digits. <http://yann.lecun.com/exdb/mnist/>.
- LeCun, Y., Bottou, L., Bengio, Y., and Haffner, P. (1998). Gradient-based learning applied to document recognition. *Proceedings of the IEEE*, 86(11):2278–2324.
- Li, L., Chu, W., Langford, J., and Schapire, R. E. (2010). A contextual-bandit approach to personalized news article recommendation. In *Proceedings of the 19th international conference on World wide web*, pages 661–670. ACM.
- Li, L., Jamieson, K., DeSalvo, G., Rostamizadeh, A., and Talwalkar, A. (2016). Hyperband: Bandit-based configuration evaluation for hyperparameter optimization. *The Journal of Machine Learning Research*.
- Lizotte, D. J., Wang, T., Bowling, M. H., and Schuurmans, D. (2007). Automatic gait optimization with gaussian process regression. In *IJCAI*, volume 7, pages 944–949.
- Martinez-Cantin, R. (2014). Bayesopt: A bayesian optimization library for nonlinear optimization, experimental design and bandits. *The Journal of Machine Learning Research*, 15(1):3735–3739.
- Mnih, V., Kavukcuoglu, K., Silver, D., Rusu, A. A., Veness, J., Bellemare, M. G., Graves, A., Riedmiller, M., Fidjeland, A. K., Ostrovski, G., et al. (2015). Human-level control through deep reinforcement learning. *Nature*, 518(7540):529.
- Mukadam, M., Dong, J., Yan, X., Dellaert, F., and Boots, B. (2017). Continuous-time gaussian process motion planning via probabilistic inference. *arXiv preprint arXiv:1707.07383*.
- Netzer, Y., Wang, T., Coates, A., Bissacco, A., Wu, B., and Ng, A. Y. (2011). Reading digits in natural images with unsupervised feature learning. In *NIPS workshop on deep learning and unsupervised feature learning*, volume 2011, page 5.
- Pedregosa, F., Varoquaux, G., Gramfort, A., Michel, V., Thirion, B., Grisel, O., Blondel, M., Prettenhofer, P., Weiss, R., Dubourg, V., Vanderplas, J., Passos, A., Cournapeau, D., Brucher, M., Perrot, M., and Duchesnay, E. (2011). Scikit-learn: Machine learning in Python. *Journal of Machine Learning Research*, 12:2825–2830.
- Ricci, F., Rokach, L., and Shapira, B. (2015). Recommender systems: introduction and challenges. In *Recommender systems handbook*, pages 1–34. Springer.

- Silver, D., Huang, A., Maddison, C. J., Guez, A., Sifre, L., Van Den Driessche, G., Schrittwieser, J., Antonoglou, I., Panneershelvam, V., Lanctot, M., et al. (2016). Mastering the game of go with deep neural networks and tree search. *nature*, 529(7587):484.
- Slivkins, A. (2011). Contextual bandits with similarity information. In *Proceedings of the 24th annual Conference On Learning Theory*, pages 679–702.
- Snoek, J., Larochelle, H., and Adams, R. P. (2012). Practical bayesian optimization of machine learning algorithms. In *Advances in neural information processing systems*, pages 2951–2959.
- Snoek, J., Swersky, K., Zemel, R., and Adams, R. (2014). Input warping for bayesian optimization of non-stationary functions. In *International Conference on Machine Learning*, pages 1674–1682.
- Snoek, J. R. (2013). *Bayesian optimization and semiparametric models with applications to assistive technology*. PhD thesis, University of Toronto.
- Song, J., Chen, Y., and Yue, Y. (2018). A general framework for multi-fidelity bayesian optimization with gaussian processes. *arXiv preprint arXiv:1811.00755*.
- Srinivas, N., Krause, A., Kakade, S. M., and Seeger, M. (2009). Gaussian process optimization in the bandit setting: No regret and experimental design. *arXiv preprint arXiv:0912.3995*.
- Sutton, R. S. and Barto, A. G. (1998). *Introduction to reinforcement learning*, volume 135. MIT press Cambridge.
- Swersky, K., Snoek, J., and Adams, R. P. (2013). Multi-task bayesian optimization. In *Advances in neural information processing systems*, pages 2004–2012.
- Thompson, W. R. (1933). On the likelihood that one unknown probability exceeds another in view of the evidence of two samples. *Biometrika*, 25(3/4):285–294.
- Vazquez, E. and Bect, J. (2007). Convergence properties of the expected improvement algorithm. *arXiv preprint arXiv:0712.3744*.

A Proofs

In all the proofs that follows, we denote $x = (z, a)$. In the case of non-contextual bandit problem, \mathcal{Z} is the empty set ϕ so $x = a$.

A.1 Proof of Lemma 1

Proof. The statement is true when $t = 1$ since a probability is non-negative. For $t \geq 2$, let $\mu_t(x) = E[f(z)|z \in p_t(x)]$. This expectation is taken with respect to the tie-breaking scheme, which is uniformly random. By Lipschitz continuity, $|f(x) - \mu_t(x)| \leq cD(p_t(x))$. Since $D(p_t(x)) \leq \frac{\alpha}{\sqrt{n_t(x)}} + l(t+1)^{-\frac{1}{d+2}}$ by our legal partition restrictions, we have, for any x ,

$$\begin{aligned} |f(x) - m_{t-1}(x)| &\leq |f(x) - \mu_{t-1}(x)| + |\mu_{t-1}(x) - m_{t-1}(x)| \\ &\leq clt^{-\frac{1}{d+2}} + \frac{c\alpha}{\sqrt{n_{t-1}(x)}} + |\mu_{t-1}(x) - m_{t-1}(x)|. \end{aligned}$$

Case 1. $n_{t-1}^0(x) > 0$:

Since the underlying function $f(x) \in [0, 1]$, it is sub-Gaussian with the sub-Gaussian parameter (at most) $\frac{1}{2}$. Since both the underlying function $f(x)$ and the Gaussian noise ϵ are sub-Gaussian, we can apply Hoeffding’s inequality:

$$\mathbf{P} \left[\left| \sum_{i=1}^n (Y_i - \mathbf{E}[Y_i]) \right| \geq u \right] \leq 2 \exp \left\{ -\frac{u^2}{2 \sum_{i=1}^n \sigma_i^2} \right\}$$

where Y_1, \dots, Y_n are independent sub-Gaussian random variables with sub-Gaussian parameter being $\sigma_1, \sigma_2, \dots, \sigma_n$.

Thus, using Hoeffding’s inequality with a change of variables, we know $|\mu_{t-1}(x) - m_{t-1}(x)| \leq \sqrt{\frac{(\frac{1}{2} + 2s^2)(4 \log t + \log 2)}{n_{t-1}(x)}}$

with probability at least $1 - \frac{1}{t^4}$. We can apply Hoeffding's inequality since the observed rewards within the same region is independent of each other. This is because the partition grows finer and we break ties uniformly randomly.

Case 2. $n_{t-1}^0(x) = 0$:

When $t \geq 2$, $|\mu_{t-1}(x) - m_{t-1}(x)| \leq \sqrt{\frac{(\frac{1}{2} + 2s^2)(4 \log t + \log 2)}{n_{t-1}(x)}}$ since $m_{t-1}(x) = 1$ and $n_{t-1}(x) = 1$. \square

Therefore we can choose $\beta_t = \alpha c + \sqrt{(\frac{1}{2} + 2s^2)(4 \log t + \log 2)}$ or $\beta_t = \Theta(\sqrt{\log t})$ to tradeoff exploration and exploitation. In addition, with probability at least $1 - \frac{1}{2t^4}$, we can remove the absolute value and bound $f(x)$ from below by

$$f(x) \geq m_{t-1}(x) - \frac{\alpha c + \sqrt{(\frac{1}{2} + 2s^2)(4 \log t + \log 2)}}{\sqrt{n_{t-1}(x)}} - c t^{-\frac{1}{d+2}}$$

or bound $f(x)$ from above by

$$f(x) \leq m_{t-1}(x) + \frac{\alpha c + \sqrt{(\frac{1}{2} + 2s^2)(4 \log t + \log 2)}}{\sqrt{n_{t-1}(x)}} + c t^{-\frac{1}{d+2}}. \quad (14)$$

A.2 Proof of Lemma 2

Proof. Recall $x_t = (z_t, a_t)$. Given context z_t , let a_t^* denote the maximizer of the reward function $f(z_t, \cdot)$. By definition of a_t , $m_{t-1}(z_t, a_t) + \frac{\beta_t}{\sqrt{n_{t-1}(z_t, a_t)}} + c t^{-\frac{1}{d+2}} \geq m_{t-1}(z_t, a_t^*) + \frac{\beta_t}{\sqrt{n_{t-1}(z_t, a_t^*)}} + c t^{-\frac{1}{d+2}} \geq f(z_t, a_t^*)$, with the second inequality holds with probability greater than or equal to $1 - \frac{1}{2t^4}$. This is due to (14) which is a consequence of Lemma 1. With probability at least $1 - \frac{1}{t^4}$ (due to the Fréchet inequalities), both $f(z_t, x_t)$ and $f(z_t, a_t^*)$ are bounded on one side. Thus the regret satisfies

$$\begin{aligned} r_t &= f(z_t, a_t^*) - f(z_t, a_t) \\ &= f(z_t, a_t^*) - m_{t-1}(z_t, a_t) + m_{t-1}(z_t, z_t) - f(z_t, a_t) \\ &\leq 2 \left(\frac{\beta_t}{\sqrt{n_{t-1}(z_t, a_t)}} + c t^{-\frac{1}{d+2}} \right). \end{aligned}$$

A non-contextual version follows by fixing z_t . \square

A.3 Proof of Lemma 3

Proof. Let F be the event that $r_t \leq 2 \left(\frac{\beta_t}{\sqrt{n_{t-1}(x_t)}} + c t^{-\frac{1}{d+2}} \right)$ for all $\lfloor \sqrt{T} \rfloor + 1 \leq t \leq T$, and we have

$$\begin{aligned} \mathbb{P}\{F\} &= 1 - \mathbb{P}\{\bar{F}\} \\ &\geq 1 - \sum_{t=\lfloor \sqrt{T} \rfloor + 1}^T \frac{1}{t^4} \\ &\geq 1 - \int_{\lfloor \sqrt{T} \rfloor}^T \frac{dt}{t^4} \\ &= 1 - \frac{1}{3 \lfloor \sqrt{T} \rfloor^3} + \frac{1}{3T^3}, \end{aligned} \quad (15)$$

where (15) is a union bound.

Now for any $T \geq 2$, with probability at least $1 - \frac{1}{3 \lfloor \sqrt{T} \rfloor^3} + \frac{1}{3T^3}$, we can bound the cumulative regret up to time

T by

$$\begin{aligned}
\sum_{t=1}^T r_t &= \sum_{t=1}^{\lfloor \sqrt{T} \rfloor} r_t + \sum_{t=\lfloor \sqrt{T} \rfloor+1}^T r_t \\
&\leq \sqrt{T} + 2 \sum_{t=\lfloor \sqrt{T} \rfloor+1}^T \left(\frac{\beta_t}{\sqrt{n_{t-1}(x_t)}} + clt^{-\frac{1}{d+2}} \right) \\
&\leq \sqrt{T} + 2\beta_T \sum_{t=\lfloor \sqrt{T} \rfloor+1}^T \frac{1}{\sqrt{n_{t-1}(x_t)}} + \int_{\lfloor \sqrt{T} \rfloor}^T clt^{-\frac{1}{d+2}} dt \\
&= \sqrt{T} + 2\beta_T \sum_{t=\lfloor \sqrt{T} \rfloor+1}^T \frac{1}{\sqrt{n_{t-1}(x_t)}} + cl \frac{d+2}{d+1} T^{\frac{d+1}{d+2}} - cl \frac{d+2}{d+1} \left(\lfloor \sqrt{T} \rfloor \right)^{\frac{d+1}{d+2}}.
\end{aligned}$$

□

A.4 Proof of Lemma 4

Proof. Following the arguments in Srinivas et al. (2009), we derive the following results. Since \mathbf{x}_t is deterministic, $H(\tilde{\mathbf{y}}_t, \mathbf{x}_t) = H(\tilde{\mathbf{y}}_t)$. Since, by definition of a Gaussian process, $\tilde{\mathbf{y}}_t$ follows a multivariate Gaussian distribution,

$$H(\tilde{\mathbf{y}}_t) = \frac{1}{2} \log [(2\pi e)^t \det (K + s_T^2 I)] \quad (16)$$

where $K = [k_T(x_i, x_j)]_{t \times t}$. On the other hand, we can recursively compute $H(\tilde{\mathbf{y}}_t)$ by

$$\begin{aligned}
H(\tilde{\mathbf{y}}_t) &= H(\tilde{\mathbf{y}}_t | \tilde{\mathbf{y}}_{t-1}) + H(\tilde{\mathbf{y}}_{t-1}) \\
&= H(\tilde{\mathbf{y}}_t | x_t, \tilde{\mathbf{y}}_{t-1}, \mathbf{x}_{t-1}) + H(\tilde{\mathbf{y}}_{t-1}) \\
&= \frac{1}{2} \log (2\pi e (s_T^2 + \sigma_{T,t-1}^2(x_t))) + H(\tilde{\mathbf{y}}_{t-1}) \\
&= \frac{1}{2} \sum_{\tau=1}^t \log (2\pi e (s_T^2 + \sigma_{T,\tau-1}^2(x_\tau)))
\end{aligned} \quad (17)$$

By (16) and (17),

$$\sum_{\tau=1}^t \log (1 + s^{-2} \sigma_{T,\tau-1}^2(x_\tau)) = \log [\det (s^{-2} K + I)]$$

For the block diagonal matrix K of size $t \times t$, let n_i denote the size of block i and B' be the total number of diagonal blocks. Then we have

$$\begin{aligned}
\det (s^{-2} K + I) &= \prod_{i=1}^{B'} \det (s^{-2} \mathbf{1}_{n_i} \mathbf{1}_{n_i}^\top + I_{n_i \times n_i}) \\
&= \prod_{i=1}^{B'} (1 + s^{-2} n_i) \\
&\leq \left(1 + \frac{s^{-2} t}{|\mathcal{P}_T|} \right)^{|\mathcal{P}_T|}
\end{aligned} \quad (18)$$

where (18) is due to the matrix determinant lemma and the last inequality is that the geometric mean is no larger than the arithmetic mean and that $|\mathcal{P}_t| \geq B'$. Therefore,

$$\sum_{\tau=1}^t \log (1 + s^{-2} \sigma_{T,\tau-1}^2(x_\tau)) \leq |\mathcal{P}_T| \log \left(1 + \frac{s^{-2} t}{|\mathcal{P}_T|} \right).$$

□

A.5 Proof of Lemma 5

Proof. Since the function $h(\lambda) = \frac{\lambda}{\log(1+\lambda)}$ is increasing for non-negative λ ,

$$\lambda \leq \frac{s_T^{-2}}{\log(1 + s_T^{-2})} \log(1 + \lambda)$$

for $\lambda \in [0, s_T^{-2}]$. Since $\sigma_{T,t}(x) \in [0, 1]$ for all x ,

$$\sigma_{T,t}^2(x) \leq \frac{1}{\log(1 + s_T^{-2})} \log(1 + s_T^{-2} \sigma_{T,t}^2(x))$$

for $t, T = 0, 1, 2, \dots$. Since the partition always grows finer, we have that for $T_1 \leq T_2$, $n_{T_1,t}(x) \geq n_{T_2,t}(x)$, and thus $\sigma_{T_1,t}^2(x) \leq \sigma_{T_2,t}^2(x)$. Now, we are ready to bound $\sum_{t=\lfloor \sqrt{T} \rfloor + 1}^T \frac{1}{\sqrt{n_{t-1}(x_t)}}$ by the sum of variances in this made-up Gaussian process. Since we require the region diameter at time t to be at least $lt^{-\frac{1}{d+2}}$ and the compact arm space $\mathcal{X} \subset \mathbb{R}^d$ has a bounded volume, the number of regions at time t is at most $l't^{\frac{d}{d+2}}$ for some constant l' . This l' takes into account the volume of \mathcal{X} and diameter of the regions in the partition. In other words, we have $B \leq l't^{\frac{d}{d+2}}$ where B is the number of regions in the partition. Suppose we query at points $x_{\lfloor \sqrt{T} \rfloor + 1}, \dots, x_T$ in the Gaussian process $\mathcal{GP}(0, k_T(\cdot, \cdot))$. Then,

$$\sum_{t=\lfloor \sqrt{T} \rfloor + 1}^T \sqrt{\frac{1}{n_{t-1}(x_t)}} \tag{19}$$

$$\leq \sqrt{T - \lfloor \sqrt{T} \rfloor} \sqrt{\sum_{t=\lfloor \sqrt{T} \rfloor + 1}^T \frac{1}{n_{t-1}(x_t)}} \tag{20}$$

$$\begin{aligned} &\leq \sqrt{T - \lfloor \sqrt{T} \rfloor} \sqrt{\sum_{t=\lfloor \sqrt{T} \rfloor + 1}^T \frac{1 + s_T^{-2}}{1 + s_T^{-2} n_{t-1}(x_t)}} \\ &\leq \sqrt{T - \lfloor \sqrt{T} \rfloor} \sqrt{\sum_{t=\lfloor \sqrt{T} \rfloor + 1}^T \frac{1 + s_T^{-2}}{1 + s_T^{-2} n_{T,t-1}^0(x_t)}} \\ &\leq \sqrt{T - \lfloor \sqrt{T} \rfloor} \sqrt{(1 + s_T^{-2}) \sum_{t=\lfloor \sqrt{T} \rfloor + 1}^T \sigma_{T,t-1}^2(x_t)}. \end{aligned} \tag{21}$$

By letting $\lambda_T = \frac{1 + s_T^{-2}}{\log(1 + s_T^{-2})}$, we have

$$\begin{aligned} (21) &\leq \sqrt{T} \sqrt{\lambda_T \sum_{t=\lfloor \sqrt{T} \rfloor + 1}^T \log(1 + s_T^{-2} \sigma_{T,t-1}^2(x_t))} \\ &\leq \sqrt{T} \sqrt{\lambda_T |\mathcal{P}_T| \log \left(1 + s_T^{-2} \frac{T - \lfloor \sqrt{T} \rfloor}{|\mathcal{P}_T|} \right)} \end{aligned} \tag{22}$$

$$\leq \sqrt{T} \sqrt{\lambda_T l' T^{\frac{d}{d+2}} \log \left(1 + s_T^{-2} \frac{T - \lfloor \sqrt{T} \rfloor}{l' T^{\frac{d}{d+2}}} \right)} \tag{23}$$

where (20) is due to the Cauchy-Schwarz inequality, (22) is a consequence of Lemma 4 and (23) is due to the fact that the function $h_\gamma(z) = z \log(1 + \frac{\gamma}{z})$ is increasing with z . Now we can set s_T to a constant and get the result. \square

Now, Theorem 1 is a natural consequence of the above analysis.